



SEISMIC RESPONSE OF NONSTRUCTURAL COLD-FORMED STEEL FRAMED INTERIOR WALL SUBASSEMBLIES WITH EXPANSION JOINTS

Y. Ji¹, K.L. Ryan¹, W. Roser¹, S.L. Wynn¹, T.C. Hutchinson², R. Belvin³

¹ University of Nevada, Reno, Reno, USA, yeji@nevada.unr.edu
² University of California, San Diego, La Jolla, USA
³ Construction Specialties Inc., Muncy, USA

Abstract: Cold-formed steel nonstructural wall subassemblies, including a variety of interior partition walls, both typical and two-hour rated shaft walls, were constructed within a 10-story mass timber building and tested at the NHERI@UC San Diego outdoor shake table. Since the primary cause of damage to cold-formed steel walls is differential story drift, the walls were detailed with two types of horizontal slip tracks to accommodate up to 2.5% of interstory drift at each level. Three types of corner expansion joints were also installed to address movement conflicts at intersecting walls. The test building was subjected to 88 earthquake motions, ranging in hazard from 43-year return period to MCE_R shaking intensities. Throughout the motions, most of the wall assemblies observed slip relative to the attached floor. Given the special detailing, the walls were isolated from the interstory drift, which reduced the drift-induced damage to the walls and door openings and shows the potential to eliminate drywall repair after large seismic events. This paper presents the relation between the measured story drift and wall slip, the special wall and joint detailing and the post-test observations of the minor damage sustained, all of which should be considered in future seismic design.

1. Introduction

Structural resilience refers to a structure's ability to reduce the damage during an earthquake and swiftly recover while sustaining its functionality and safety (Bruneau and Reinhorn 2006). In addition to the resiliency of structural systems, nonstructural components also play a critical role in enhancing the overall resilience of a building. Improving the performance of nonstructural elements helps to not only prevent injuries and property damage, but also contributes to the uninterrupted functionality of essential services during and after an earthquake event. However, damage to some nonstructural components occurs at small interstory drift ratios (e.g. Taghavi and Miranda 2003); among these components, cold-formed steel (CFS)-framed interior partition walls, constructed floor to floor, are susceptible to damage by interstory drift. Due to the widespread use of CFS-framed partition walls, the damage and economic loss they sustain during an earthquake will be significant (Davies et al. 2011). Damage is expected to initiate at interstory drifts of 0.1% - 0.2% for typical full height partition walls (Bersofsky 2004), considerably lower than for primary structure. When the interstory drift level increases to 2%, the costs to repair partition walls will equal their construction cost (Lee et al. 2007).

CFS-framed partition walls consist of vertical studs spaced 406.4 mm or 609.6 mm o.c. between top and bottom tracks and sheathed with drywall on both sides (AISI 240-20 2020). Commonly, the studs are screwed to the tracks, and the tracks are fully connected to the floor slab above and below. Thus, the connections between the studs to tracks and tracks to floor slabs are easily damaged when subjected to seismic interstory drifts. To understand this damage, a variety of experiments have been undertaken. Early studies include the work of Rihal (1982), who performed cyclic tests of 14 planar partition walls, and Serrette et al. (1997), which aimed at comparing panel connection-scale tests with full-scale racking tests on a blend of structural and nonstructural CFS-framed walls. These tests were amongst the earliest to develop damage state definitions

and seismic fragilities for partition walls. More recent efforts expanded to understand the implications of partition walls within a building setting. For example, CFS-framed interior partition walls and shaft walls were included in a shaking table test of a 5-story full scale building (Wang et al. 2015). In this test, the interior partition walls were not damaged when the building was in the seismically-isolated configuration. However, when the primary building was fixed to the shake table, the interior partition walls were damaged at low interstory drifts consistent with prior wall-only test findings, namely at about 0.10%.

In practice, the damage to CFS-framed interior partition walls can be minimized through a variety of practical approaches. For example, one option may be to strengthen the partition walls and their associated connections such that they are more resistant to large seismic-induced loads - this naturally stiffens the wall and reduces deformations and associated damage. However, while improving the strength, the gypsum boards still exhibit brittle behavior under very low deformation. Another option is to isolate the partition walls from interstory drift. To address this approach, various slip or sliding track details have been proposed and are used by the industry. In the basic slip track detail, studs are not connected to the track at the top of the wall, and slip occurs between the studs and the track (Davies et al. 2011). However, in tests with such details, damage occurred at the ends of the wall due to the studs popping out from the end of the track (Retamales et al. 2013). To solve this problem, several innovative track details were investigated. The double slip track detail (Fig. 1a) uses nested tracks at the top. The upper track is connected to the floor slab, and the lower track is connected to the study so that slip occurs between the two tracks. In addition, the gap between the upper and lower track provides 19 mm movement in the vertical direction. The double slip configuration was superior to the conventional slip track in holding the wall together under significant drift (Hasani and Ryan 2021). Araya-Letelier et al. (2019) proposed a sliding connection detail consisting of an upper track sandwiched between a thin steel plate attached to the top slab and a rectangular short steel tube. In addition, the upper track had large circular holes to accommodate the relative sliding deformations between the top of the partition wall and the slab in in-plane and out-of-plane directions. This detail performed well up to the drift limits provided by the holes but was not favored by industry due to the difficulty of manufacturing the tracks. However, applying a closely related concept, a proprietary product (Fig. 1b) uses a horizontally slotted top track wherein screws are not fully tightened to the slab above. The slots allow the top track to slide ±76.2 mm relative to the floor in the in-plane direction. Moreover, the vertical slots in the flange can provide 19 mm movement in the vertical direction. To the author's knowledge, this solution has no publicly available test data.

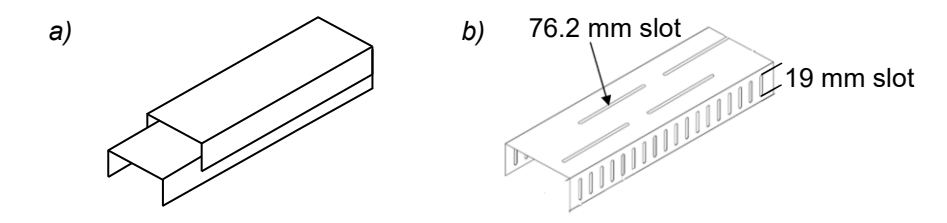


Figure 1. (a) Double slip track and (b) proprietary slotted slip-track (CEMCO, 2023)

The benefit of incorporating a slip track can be diminished due to incompatibilities at intersecting or return walls. A few solutions have been proposed to separate the movement of the intersecting in-plane and out-of-plane walls. In the corner gap detail, the tracks are discontinued and the nearest studs are located 50.8 mm from the intersection so that the wall can penetrate the corner region (Davies et al. 2011, Retamales et al. 2013, Hasani and Ryan 2021). In the flexible corner detail, the top track screws are removed within 600 mm of wall intersections to allow drift incompatibility to be absorbed by bending of the out-of-plane wall (Retamales et al. 2013, Mulligan et al. 2020). Finally, Hasani and Ryan (2021) considered 13 mm commercial expansion joints, often installed for thermal or other types of movement, near the corner region to absorb some of the drift incompatibility. Such systems have proven worthy in single and two-story wall models.

To this end, a shake table test of a 10-story mass timber building at NHERI@UC San Diego in 2023 provided the opportunity to investigate the CFS-framed interior partition walls. A variety of wall assemblies, including typical partition walls and shaft walls, were constructed on stories 4 through 6 of this building specimens. All interior walls included a top of wall horizontal slip detail and were designed to accommodate interstory drift ratios up to 2.5%. In addition, details included three types of expansion joints that were installed and tested as part of the program to reduce interstory drift damage. The primary objective of this paper is to evaluate the

response of these CFS-framed interior partition walls, and specifically whether these innovative details can reduce the drifts realized by the partition walls and subsequently reduce the damage.

2. Test Program

2.1. Test Building

The test building, a full-scale 10-story mass timber building, was built on the NHERI@UC San Diego outdoor shake table (Fig. 2a). This 10-story test building incorporated resilient post-tensioned mass timber rocking wall lateral systems (cross-laminated timber (CLT) and mass plywood panel (MPP) with U-shaped flexural plates (UFPs)). In addition, gravity connection details - pinned connections at veneer-laminated timber (VLT) beams and columns - were designed to remain damage-free during a series of shaking. The total height of the test building was 34.3 m, with each story being 3.3 m, except story 1, which was 3.9 m. The floor plan of the building was roughly 10 m x 10.5 m. The test building also included other nonstructural systems such as exterior façade subassemblies (CFS-framed with an aluminum composite exterior finish and curtain walls on stories 1-3) and a full-scale stair tower with access on all floor levels (Fig. 2b).



Figure 2. Test building: (a) 10-story mass timber building; (b) nonstructural systems

2.2. CFS-framed Partition Wall Subassemblies

Various interior wall subassemblies with CFS framing were installed into the test building on stories 4 through 6; these floors were selected as they are unaffected by exterior non-structural façade testing and accessibility. Two types of interior walls were used throughout these three stories, namely: partition walls and shaft walls. The partition walls, shown schematically in Fig. 3a, were constructed with typical studs connected to top and bottom tracks; the top-of-wall detail incorporated either the double slip track or proprietary slotted slip-track (hereafter referred to as "slotted slip") (Fig. 1). Typical framing sizes are denoted in Fig. 3a. Both double slip track and slotted slip track allowed 76.2 mm movement in both in-plane directions. The walls were sheathed with 15.9 mm thick gypsum board on both sides. To allow for free track slip, the construction details for these two types of slip track were emphasized to the contractors. For the double slip track, drywall screws installed across the slip joint can prevent proper slip. The slotted slip track is easier to build in principle, but the screw attached to the upper floor must not be overtightened.

In contrast, the shaft walls, shown in Fig. 3b, were assembled with fire rated J-track 101.6 mm web and CH studs 101.6 mm web. The studs and a 25.4 mm thick shaft liner board was friction fit into the interior or shaft side of the wall, and the exterior side was sheathed with two layers of 15.9 mm gypsum board. Thus, the shaft wall can also slip in the in-plane direction. The boundary members of the two types of interior partition wall assemblies were attached to the wood floor slabs above and below with heavy duty 6.35 mm diameter x 50.8

mm long screws. These fasteners were spaced at 406.4 mm o.c. at the boundaries, whereas the spacing at the top tracks was 203.2 mm o.c. In addition, the stud-to-track connections were provided by #8 sheet metal screws, while #8 self-drilling drywall screws were used to attach the gypsum boards to the studs.

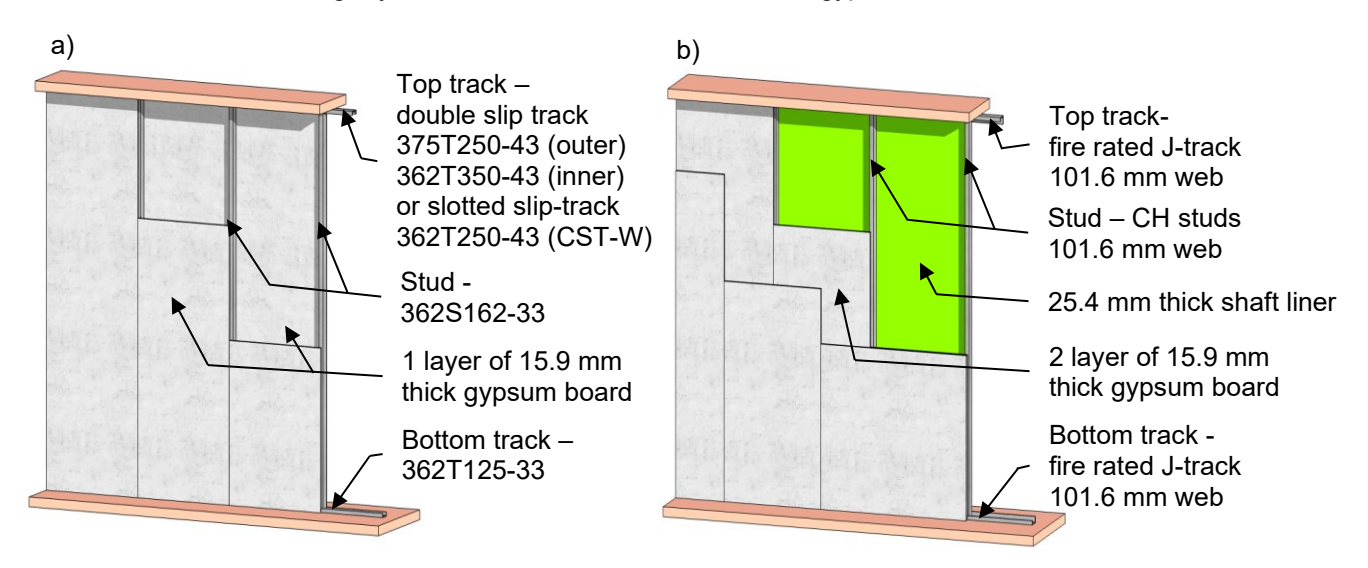


Figure 3. Details of interior partition walls: (a) partition wall; (b) shaft wall

Plan layouts for levels 4 through 6 are shown in Fig. 4. The wall layouts on Stories 4 and 5 (Fig. 4a and 4b) were conceived to represent a residential floor plan, and then simplified to fit on the minimal size building footprint. Story 4 incorporated interior partition walls that extend to the shaft wall assembly, which wrapped around the central stair core in all directions. Story 5 had a similar layout to Story 4, however the stairwell, a 10-story prefabricated steel Modular Stair System tower had a built-in shaft wall. W1, W3, W5, W6, W8 and W10 incorporated the double slip track and were 2.4 m long, while W1, W3, W7 and W9 were detailed as slotted slip and were 1.8 m to 2.1 m long. On story 4, W11 to W14 were shaft walls ranging from 3.6 m to 4.8 m in length. Hollow metal doors (1 m wide by 2.2 m high) included variations on frames, locks and hardware and were installed in W1 to W3, W5 to W8, and W10 and W11. In addition, 362T125-43 headers and 362S162-43 jamb studs were utilized at the door openings. Besides the residential floor plans, two independent wall configurations were built on Story 6 (Fig. 4c). A C-shaped wall (W15) with segments 1.7 to 1.8 m long and a T-shaped wall (W16) with segments 1.5 m and 3 m long were built on the northeast and northwest sides, respectively.

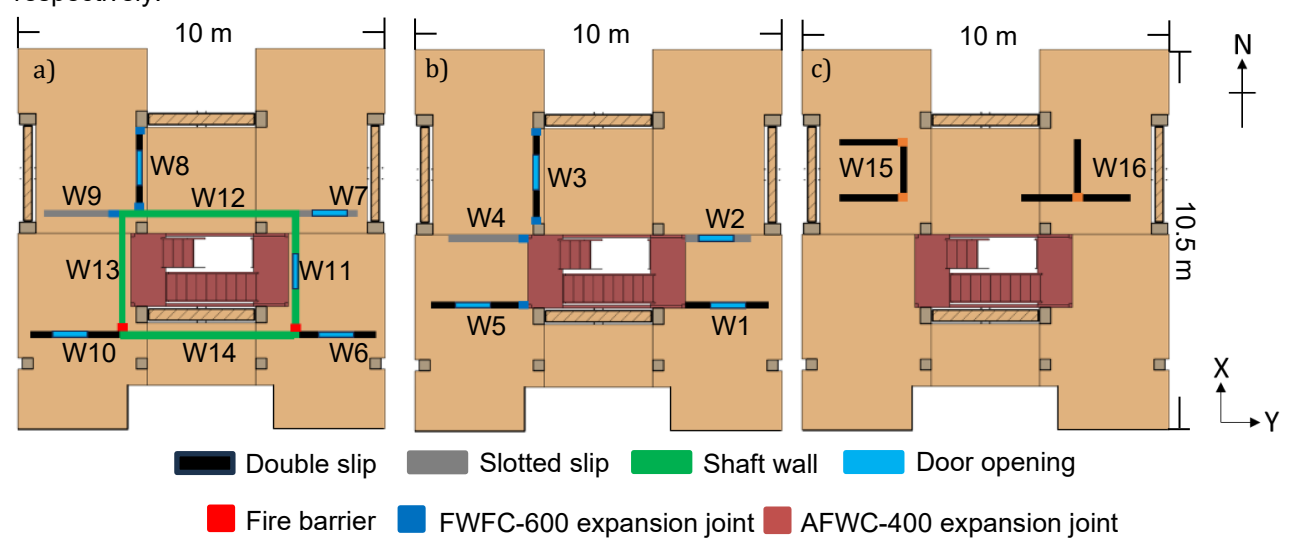


Figure 4. Interior wall plan: (a) Story 4 residential floor plan with shaft walls, (b) Story 5 residential floor plan, (c) Story 6 independent wall floor plan

2.3. Wall Intersection Details

Expansion joints with commercial joint were applied at many intersection locations (Fig. 4) to separate the movement of adjacent out-of-plane walls from in-plane walls (Construction Specialties, 2023). Several locations used the FWFC-600 expansion joint cover (Fig. 5a) that uses rubber (Santoprene) gaskets fit into extruded aluminum frames to accommodate 102 mm of relative movement in each direction. At the intersecting corner of the shaft wall and partition wall, the fire rating of the shaft wall should be maintained. Here, the RFX-4W fire barrier, made of a compressible fire-resistant material, was inserted into the joint to separate the movement of the in-plane and out-of-plane segments of the shaft wall (W13 to W14 and W11 to W14 connection) (Fig. 5b). While the slip mechanisms are different, the outer top track of W10 and W6 and the Fire Rated J-Track of W14 were notched to allow the aligned interior wall and shaft wall segments (W10, W14 and W6) to move together. In addition, standard corner details were applied in some locations for a direct comparison to the innovative solutions. Story 6 utilized a different type of expansion joint, the AFWC-400 joint (Fig. 5c), which has formed aluminum cover plates that fit over extruded aluminium frames.

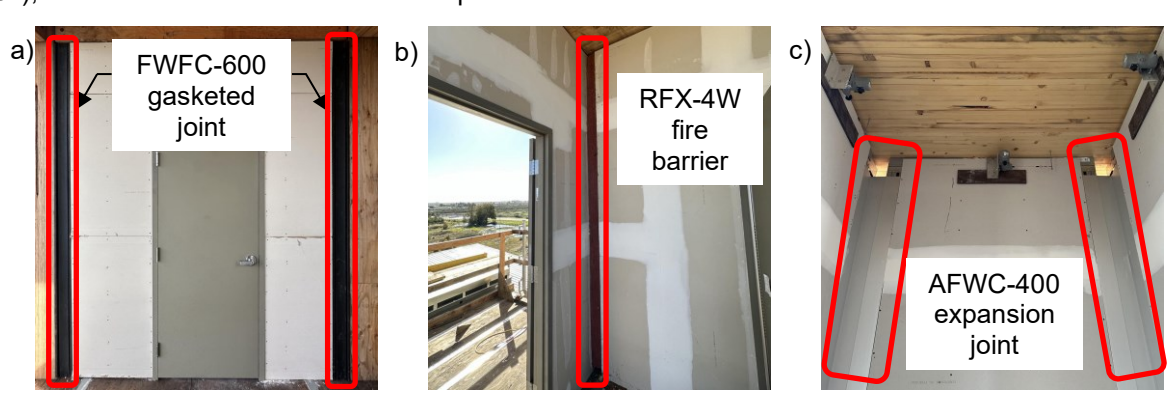


Figure 5. Commercial expansion joint covers: (a) W3, FWFC-600 gasketed joint, (b) W11, RFX-4W fire barrier, (c) W15, AFWC-400 expansion joint

2.4. Instrumentation and Earthquake Test Motions

To monitor the behavior of the interior partition walls, the following three types of sensors were installed:

- 1) Accelerometers were used to monitor the horizontal and vertical acceleration of the walls. These were installed on cubes, which were mounted into the wall (e.g. Fig. 6a).
- 2) String potentiometers (string pots) and linear potentiometers (linear pots) were used to measure the relative horizontal slip between the wall and the upper floor. For a string pot, one side was connected to the upper slab and the other side was connected 127 mm below the top of the wall, as shown in Fig. 6b. String pots were also used to monitor the displacement across the intersecting wall expansion joints. These string pots were connected to the wall on each side of the joint.
- 3) Linear pots were used for smaller movements (76.2 mm to 127 mm movement), such as most shaft walls on level 4, and the east walls on level 5, which lacked expansion joints (Fig. 6c).

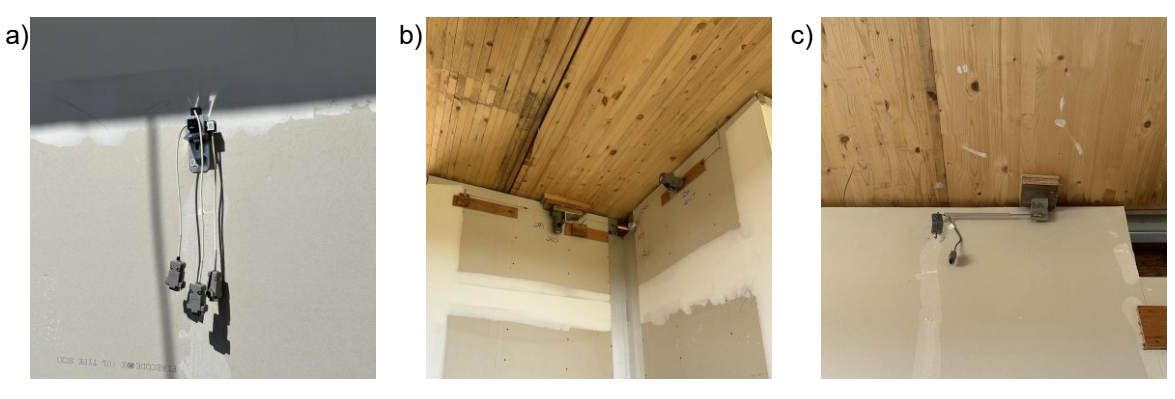


Figure 6. Sensors installed: a) accelerometers, b) string pots at top of the wall and the corner joint, c) linear pots at top of the wall.

The test program consisted of 88 earthquake motions scaled from 43-year return period to risk-targeted maximum considered earthquake (MCE_R) shaking intensities. The displacement of the floor was calculated by double integrating the center of mass recorded acceleration. The interstory drift was computed as the difference of displacement of the two adjacent stories. Then, the peak interstory drift ratio (PIDR) was computed as the absolute maximum interstory drift over the normalized story height. A subset of motions has been chosen to represent the range of intensities and multi-directional variations applied, with an emphasis towards studying the response due to the larger intensity tests. The earthquake input motions and computed peak interstory drifts for the selected motion subset are summarized in Table 1. All records were amplitude scaled to best match the target spectrum at each hazard level. The maximum PIDR in the east-west (X) direction on stories 4, 5 and 6 are 1.61%, 1.41%, and 1.72%, respectively. The maximum PIDR in north-south (Y) direction on stories 4, 5, and 6 are 1.44%, 1.95%, and 1.58%, respectively. Complete information about the ground motion records selected, scaling methodology, and the full suite of tests is provided in Wichman (2023).

Table 1. Summary of selected earthquake motion and peak interstory drift

Test ID	Hazard Level	Earthquake event - Direction	PIDR (%)					
			Story 4		Story 5		Story 6	
			X	Y	X	Υ	X	Υ
44	475	Northridge - XYZ	0.59	0.62	0.58	0.80	0.70	0.69
46	475	Chi-Chi - XY	0.78	0.83	0.87	1.14	0.91	0.91
56	43	Ferndale - XYZ	0.10	0.11	0.09	0.17	0.12	0.13
59	225	Ferndale -XY	0.36	0.36	0.36	0.46	0.43	0.47
62	225	Tohoku - XY	0.37	0.44	0.34	0.61	0.40	0.55
69	225	Niigata, Japan - XYZ	0.30	0.33	0.37	0.41	0.36	0.42
70	475	Chi-Chi - X	0.86	0.06	0.81	0.13	0.92	0.04
71	475	Chi-Chi - Y	0.10	0.83	0.18	1.12	0.15	0.89
<i>75</i>	475	Ferndale - XYZ	0.58	0.49	0.65	0.58	0.70	0.69
76	475	Tohoku -X	0.47	0.05	0.41	0.09	0.53	0.03
77	975	Northridge - X	0.98	0.05	0.98	0.12	1.18	0.04
78	975	Northridge - Y	0.10	0.75	0.14	1.09	0.11	1.01
79	975	Northridge - XY	1.02	0.76	1.09	1.01	1.16	1.03
81	475	Chi-Chi - XYZ	0.82	0.79	0.87	1.12	0.90	0.90
82	975	Tohoku - X	0.90	0.06	0.84	0.15	0.99	0.05
86	975	Northridge - XYZ	1.07	0.77	1.05	1.02	1.12	1.05
87	975	Ferndale - XYZ	0.79	0.55	0.73	0.73	0.91	0.76
88	MCE_R	Loma Prieta - XYZ	0.80	1.44	0.69	1.95	0.80	1.58
90	MCE_R	Ferndale -XYZ	1.00	0.76	1.04	0.94	1.17	0.98
91	975	Tokachi - X	1.61	0.10	1.41	0.32	1.72	0.13
92	975	Victoria, Mexico - XYZ	1.16	0.87	1.10	1.13	1.38	1.26
93	MCE_R	Tohoku - X	1.43	0.09	1.30	0.26	1.51	0.10

3. Observations of the Response of CFS- framed Interior Walls

The performance of the interior partition walls when subjected to earthquake shaking was evaluated by documenting physical damage and correlating this with processed analog measurements. Observed physical damage was documented by videos and photos taken during visual inspections periodically following select tests. These inspections were focused on the gypsum board and expansion joints as the wall framing generally was not visible. In addition, none of the interior partition walls were repaired during the test. Therefore, all observed damage to the walls was cumulative damage. Drift across the wall was computed as the difference between the interstory drift and the measured wall slip. Due to uncertainty in the interstory drift, the peak wall drift is likely to be an overestimate.

3.1. Comparison of Double Slip Track, Slotted Slip Track and Shaft Wall

Figure 7 compares derived interstory drift, measured wall slip, and derived resultant drift to the partition wall for W4 (slotted slip detail) and W5 (double slip detail) subjected to MCE_R Ferndale XYZ. Both the slotted slip and double slip detail were effective, which means that the construction details were built to specification. The maximum slip on W4 was 44.8 mm, while on W5 was 38.2 mm. In addition, the PIDR for Story 5 was computed to be 1.04% (35 mm), and thus the maximum drift of the wall was computed to be about 0.3% (10 mm) in the opposite direction of slip. The results suggest that the PIDR on Story 5 was underestimated, and the authors acknowledge the inherent uncertainty in deriving story drifts by double integrating the recorded accelerations.

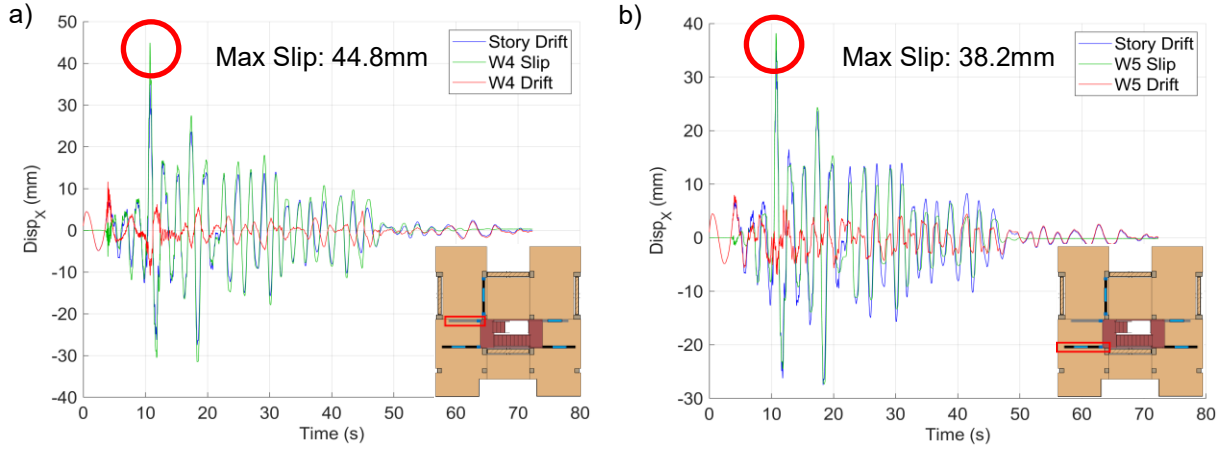


Figure 7. Story 5 slip comparison: (a) W4 with slotted slip track and (b) W5 with double slip track for Test 90: MCE_R Ferndale XYZ

The end gypsum cover panels of the walls with the double slip track detail were damaged during the test, as shown in Fig. 8. This damage was only observed in the double slip detail due to the in-plane movement. The top of the end wall gypsum cover impeded the top track movement after the wall slipped, as shown in Fig. 9. However, this damage is easy to repair, or can be prevented by trimming the end of the wall gypsum lower than the upper track (by 63.5 mm), and any exposed ends would likely be hidden in the ceiling plenum.

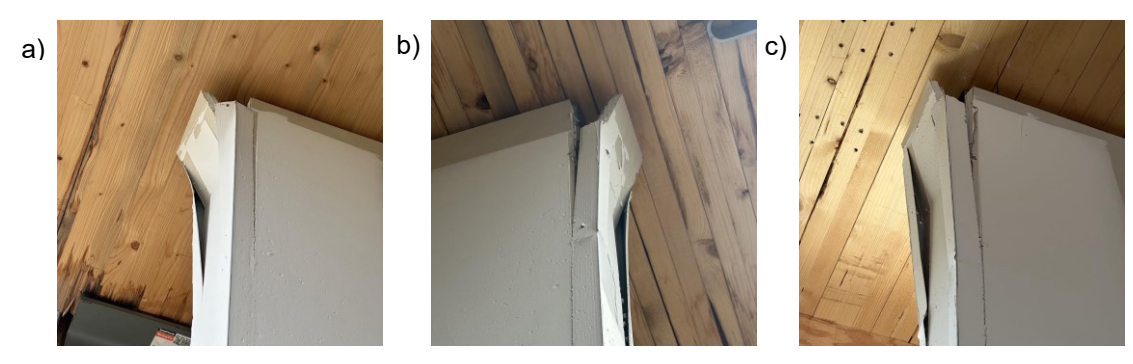


Figure 8. End of wall panel damage: (a)W6, (b) W5, (c) W16

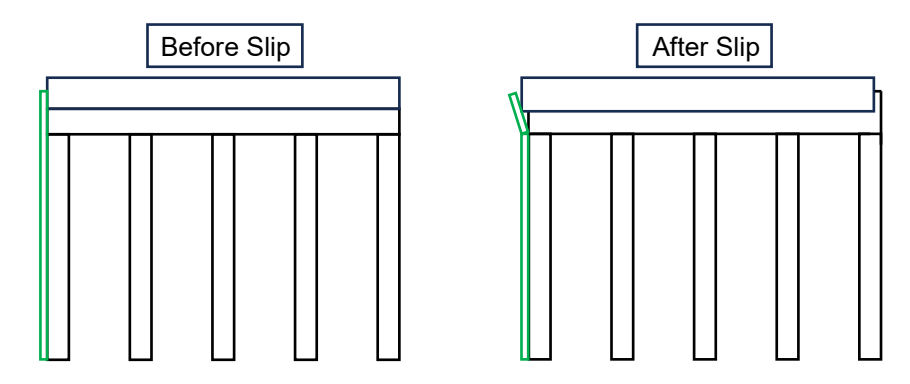


Figure 9. Concept of the end wall panel damage on the double slip track.

Shaft walls W11 and W13 also slipped up to 25.4 mm during the tests. The detailing strategy used at W13 to W12 and W11 to W12 intersections was effective. Although no expansion joint was used, the details were to "unfix" the exterior gypsum boards at the ends and add 25.4 mm gap between the end shaft liner and the end stud to accommodate the in-plane movement. For W6 and W10 to W14 connections, the detail called to cut 127 mm off the partition and shaft walls' top track flanges to avoid collision with the end studs of the adjacent wall. Moreover, the partition and shaft wall end studs were screwed together to induce the two types of walls to slip together. Figure 10 shows that the W14 shaft wall (Fig. 10b) moved almost identically with the W10 partition wall (Fig. 10a), up to 29.3 mm.

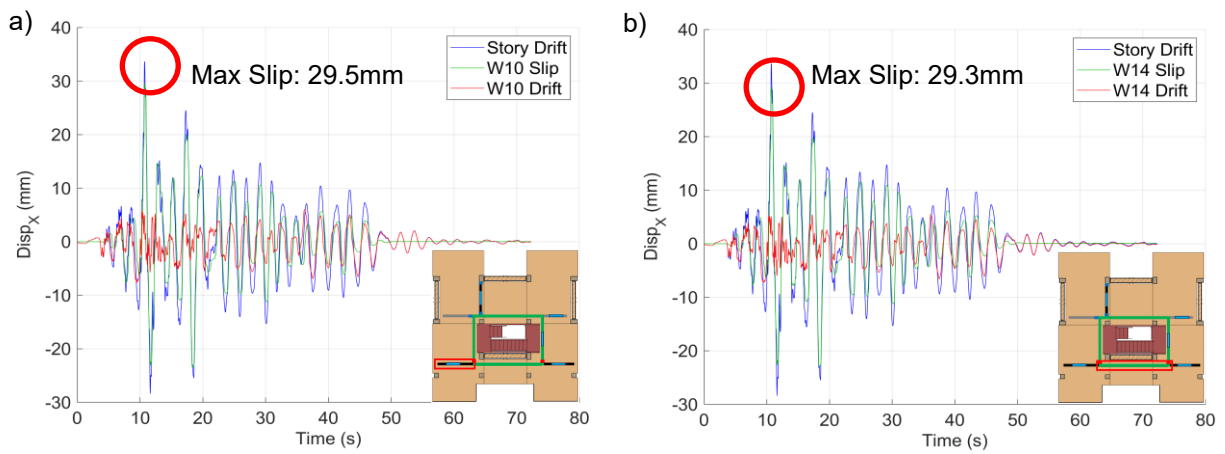


Figure 10. Story 4 slip comparison: (a) W10 with double slip track and (b) W14 with shaft wall for Test 90: MCE_R Ferndale XYZ

3.2. Effectiveness of Different Joints

Next, the effectiveness of the different types of joints is examined. All types of joints (FWFC, AWFC and RFX fire barrier) accommodated some movement, but much greater slip and corresponding joint movement occurred in some locations compared to others. Mentioned previously, W4 and W5 both incorporated FWFC joints, which were effective in these locations (Fig. 7). On the 4th story, FWFC joint was installed between W9 and W12. In 975 Tokachi X, W9 slipped 13 mm, which was lower than expected (Fig. 11a), while W12 slipped nearly 53.1mm in the same motion (Fig. 11b). In other words, W9 and W12 slipped independently, and the difference movement of the walls were accommodated by FWFC joint. On the 5th story, W5 with the FWFC expansion joint slipped considerably in both directions (up to 69.5 mm, Fig. 12a). In contrast, Wall W1, without a joint, slipped more than 60 mm in one direction but only 23.2 mm in the other (Fig. 12b). This one-sided slip was observed because the wall joint was free to open, but could close or move at most 25.4 mm before impacting with a stair tower gravity column. On story 6, the AFWC joint accommodated the incompatible movement at the corner region, as shown in Fig. 13a and 13b. Finally, the RFX fire barrier was observed to accommodate movement across the joint; however, the movement was not measured.

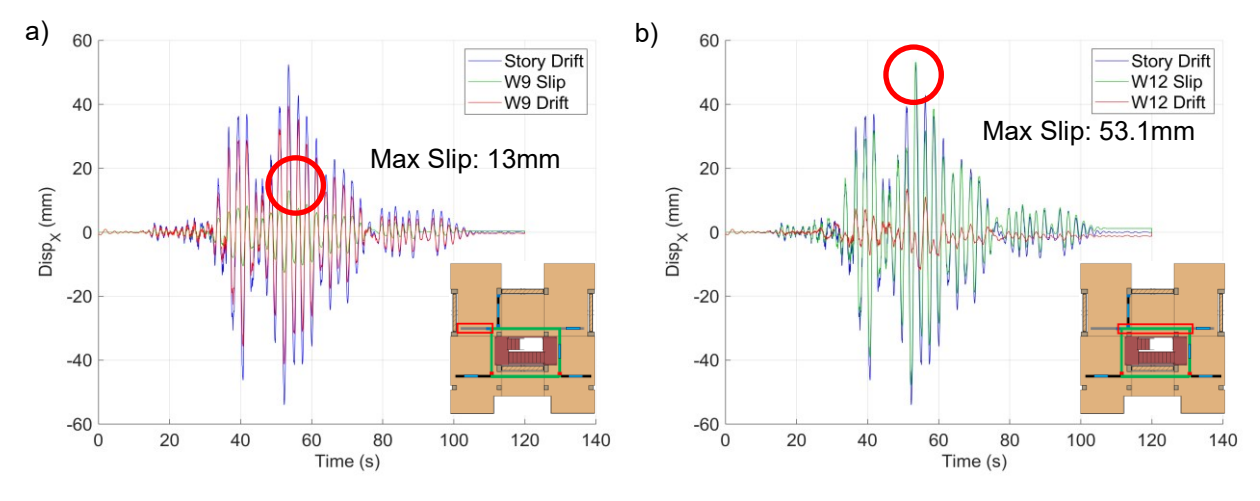


Figure 11. Story 4 slip comparison: (a) W9 (b) W12 for Test 91: 975 Tokachi X

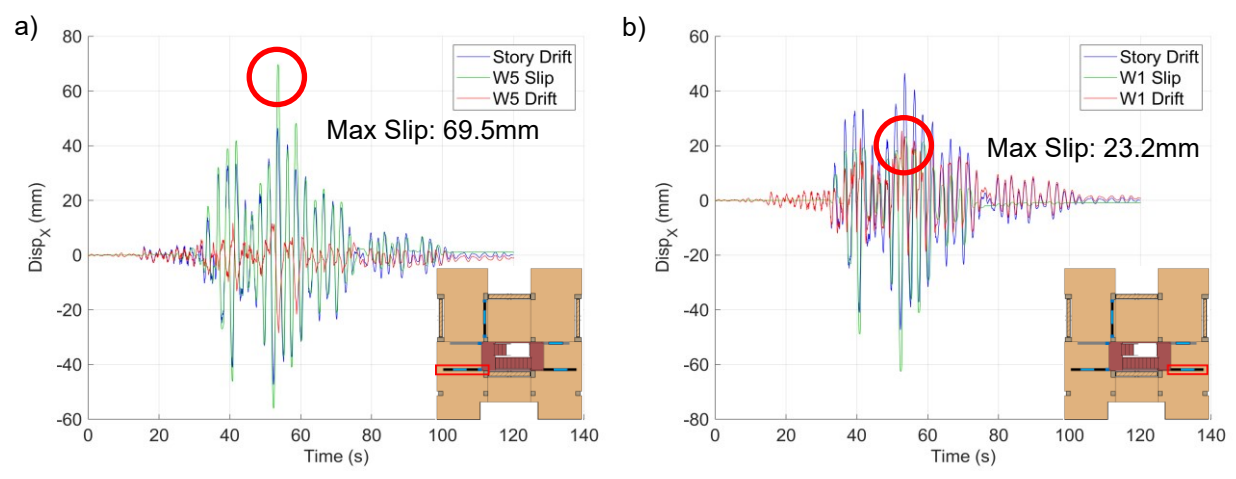


Figure 12. Story 5 slip comparison: (a) W5 (b) W1 for Test 91: 975 Tokachi X

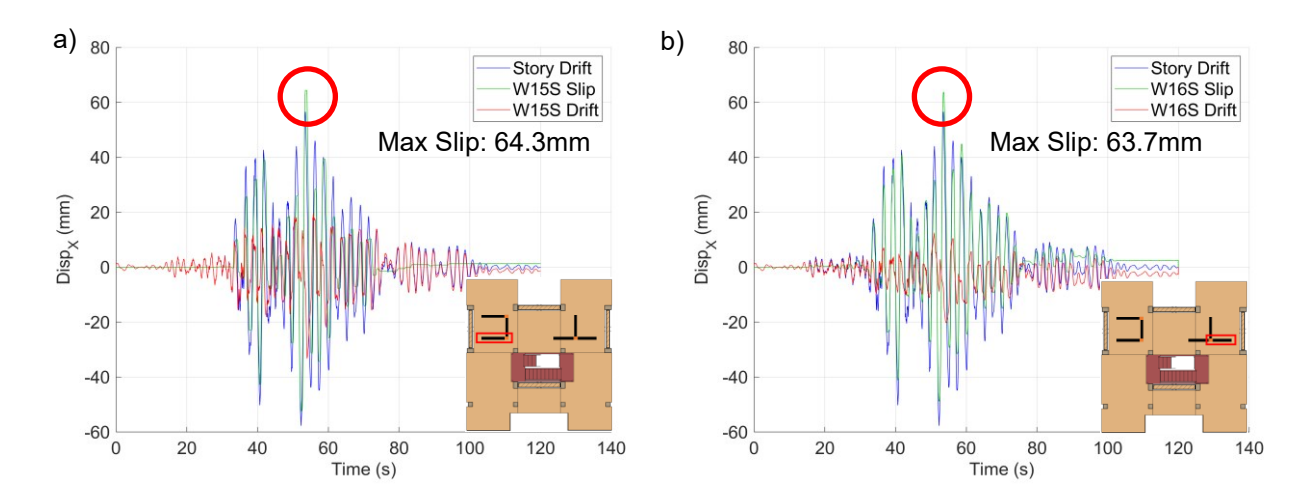


Figure 13. Story 6 slip comparison: (a) W15 (b) W16 for Test 91: 975 Tokachi X

3.3. Damage Observation

The primary observed damage to the interior partition walls is summarized in Fig. 14 to 16. On story 4, Figures 14a and 14b show that the joint tape started to crack in some walls at story drifts of approximately 0.34%. At W9, the end of the wall corner bead was damaged due to insufficient space between the wall and the upper-level floor (Fig. 14c). At W8, due to difficulty of installing the supplied hardware in the studs, the expansion joint hardware screws reflected incipient pull out and ultimately completely pulled out of the aluminum liners that house the gaskets at drifts of 0.57% and 1.44% respectively (Fig. 14d and 14e). The correct screws for the substrate should be installed every 457.2 mm o.c for future construction to avoid this type of failure. Figures 14f to 14i show that the end of the wall at W11 cracked as it was not separated from the incompatible movement from the adjacent wall. On story 5, several examples of damage at the wall-stair column intersections that lacked official expansion joints are shown in Fig. 15. On story 6, Figure 16 shows that the expansion joint covers at W15 and W16 on story 6 were bent and popped out due to the bidirectional movement putting torque demand on the joint cover. The movement that led to this phenomenon is illustrated in Fig. 17.

4. Conclusions

Cold-formed steel framed interior wall subassemblies were installed on Stories 4 to 6 in a full scale 10 story timber test building and subjected to a series of earthquake motions ranging from 43-year return-period to MCE_R shaking intensities. These interior wall subassemblies were designed with different drift compatible details, including top slip joints and expansion joints at intersecting walls, to reduce the damage caused by interstory drift. Story 4 incorporated partition walls that extend to the shaft wall assembly around the central



Figure 14. Observed damage to partition walls and expansion joint on Story 4 at various stages of testing.

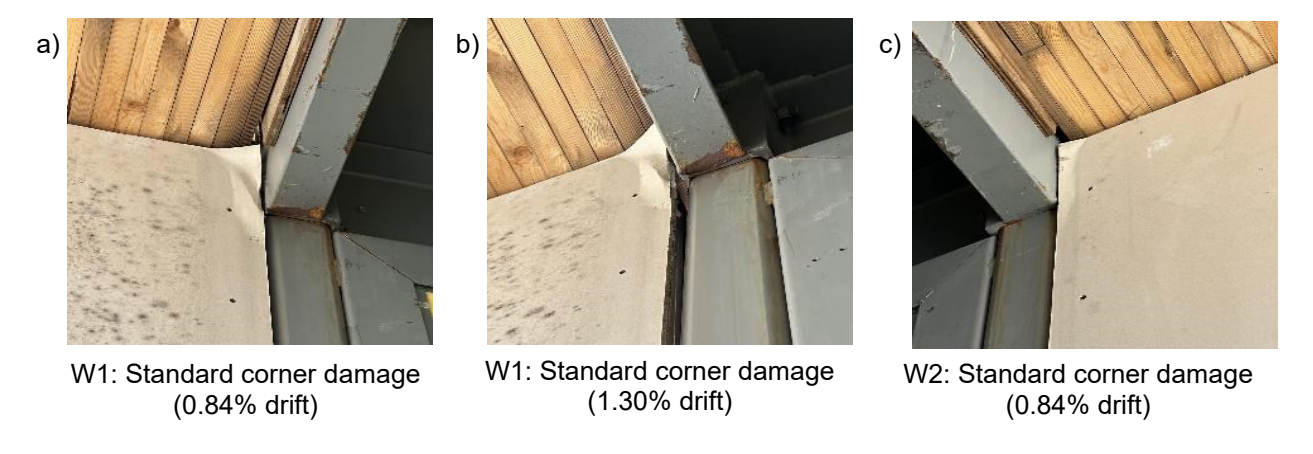


Figure 15. Observed damage to partition walls on Story 5 at various stages of testing.

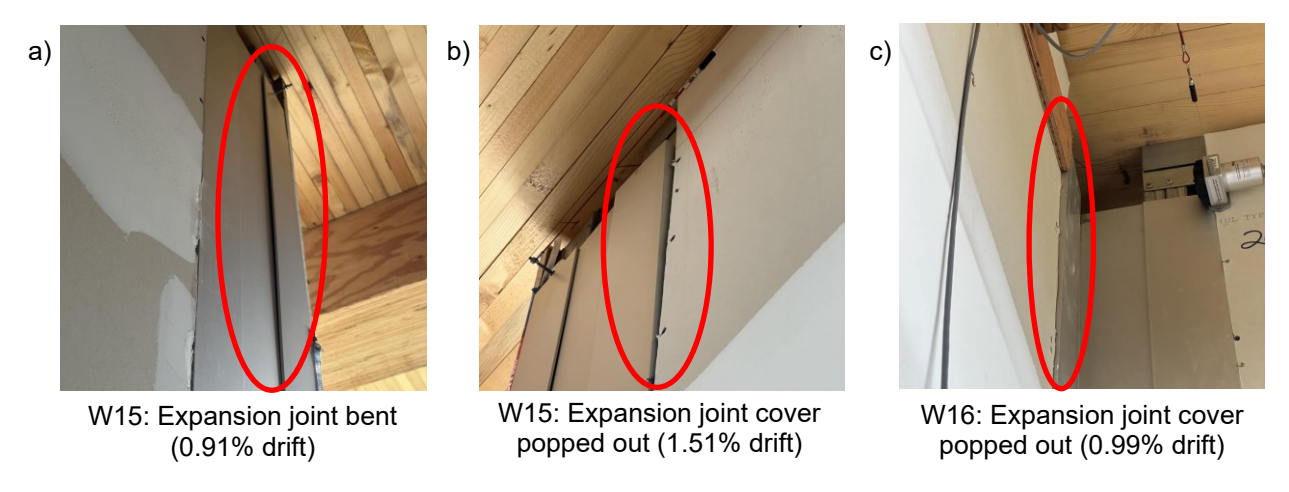


Figure 16. Observed damage to expansion joints on Story 6 at various stages of testing.

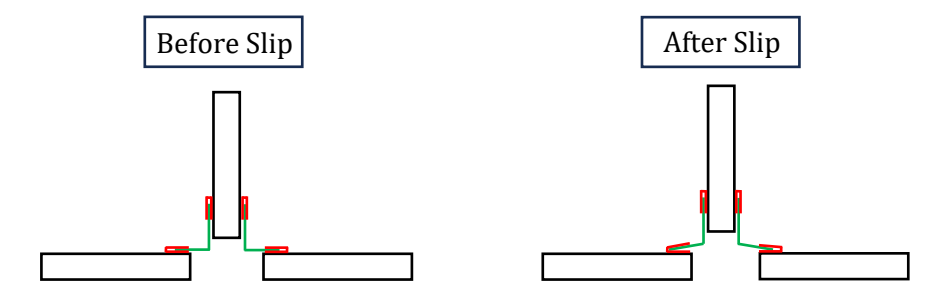


Figure 17. Concept of the expansion joint damage at story 6, specific to W16.

stair core from all directions. Story 5 had the same configuration, but the shaft wall was integral to the prefabricated modular stair system. Story 6 focused on the performance of a different type of corner expansion joint and considered a C and T arranged interior partition wall. The main findings from this shake table test program are summarized as follows:

- Both slip track details, the slotted track and the double slip track, worked well during the shake table program. Moreover, the details of tying the intersecting partition wall and shaft wall together worked perfectly. However, damage occurred at the end panel of double slip track due to the collision with the outer track flange. This damage could be prevented by stopping the end panel gypsum board short, i.e. below the slip joint, pending conformance with fire rated wall requirements.
- All of the expansion joints considered in this building specimen (FWFC, RFX Fire Barrier, and AFWC) accommodated movement across the joints, although some variations were observed. On stories 4 and 5, the walls with the FWFC-600 expansion joint slipped independently to the adjacent wall or stair column. On Story 6, the AFWC-400 expansion joint separated the movement of the adjacent walls, but when subjected to larger drifts the joint covers were bent due to the torque demand from the bidirectional movement.
- The standard corner details used in this test did accommodate some movement, as damage was not noticeable at the very low drifts (less than 0.5%), which was otherwise apparent in previous test programs. On Story 4, the standard corner detail prevented W12 from slipping; thus, the gypsum cracked at the adjacent wall W11. In Story 5, both W1 and W2 without joints were ultimately damaged due to interaction with the stair hardware.
- All physical damage observed in these tests are readily repairable, thus characterized as minor damage. Moreover, slight construction modifications may easily mitigate the damage that was observed.

5. Acknowledgements

The structural system scope of NHERI TallWood Project is sponsored by NSF Grants No. CMMI-1635227,

1634628, 1634204. The use and operation of NHERI shake table facility is supported by NSF Grant No. CMMI-1520904. The nonstructural component scope of this project was sponsored by NSF Grant No. CMMI-1635363, USFS Grant No. 19-DG-11046000-16, Softwood Lumber Board, Computers and Structures Inc, the GAANN Fellowship Program at UNR, and other industry sponsors. Materials and in-kind support for the wall subassemblies discussed in this paper are provided by CEMCO® Steel, Construction Specialties, Simpson Strong-tie, and USG. The modular stair system with integrated shaft walls was provided by Construction Specialties. The authors are indebted to the many contributors that made this project possible. Any opinion, findings, and conclusions or recommendations expressed in this material are those of the authors and do not necessarily reflect the views of the National Science Foundation nor any industry partner or other sponsors.

6. References

- AISI 240-20 (2020). North American Standard for Cold-Formed Steel Structural Framing, American Iron and Steel Institute, Washinton, DC, 2020.
- Araya-Letelier G., Miranda E., and Deierlein G. (2019). Development and Testing of a Friction/Sliding Connection to Improve the Seismic Performance of Gypsum Partition Walls. *Earthquake Spectra* 35 (2): 653-677. DOI: 10.1193/123117EQS270M.
- Bersofsky A. (2004). A Seismic Performance Evaluation of Gypsum Wallboard Partitions. MSc Thesis, University of California at San Diego, San Diego, CA.
- Bruneau M. and Reinhorn A. (2006). Overview of the Resilience Concept. *Proceedings of the 8th U.S. National Conference on Earthquake Engineering*, USA, 18–22 April.
- CEMCO (2023). CST Slotted slip track. Accessible at: https://cemcosteel.com/product-category/steel-framing-cst-slotted-tracks/
- Construction Specialties (2023). Expansion joints. Accessible at: https://www.c-sgroup.com/expansion-joint-solutions.
- Davies R. D., Retamales R., Mosqueda G., and Filiatrault A. (2011). Experimental Seismic Evaluation, Model Parameterization, and Effects of Cold-Formed Steel-Framed Gypsum Partition Walls on the Seismic Performance of an Essential Facility. Tech. Rep. MCEER-11-0005, Buffalo, NY.
- Hasani H., Ryan K.L. (2021). Experimental Cyclic Testing of Reduced Damage Detailed Drywall Partition Walls Integrated with a Timber Rocking Wall. *Journal of Earthquake Engineering* 26 (10): 5109-5129. DOI: 10.1080/13632469.2020.1859005
- Lee T.-H., Kato M., Matsumiya T., Suita K., and Nakashima M. (2007). Seismic Performance Evaluation of Non-structural Components: Drywall Partitions. *Earthquake Engineering & Structural Dynamics* 36 (3): 367–382. DOI: 10.1002/eqe.638.
- Mulligan J., Sullivan T.J., & Dhakal R.P. (2020). Experimental Seismic Performance of Partly-Sliding Partition Walls. *Journal of Earthquake Engineering* 26 (3): 1630-1655. DOI: 10.1080/13632469.2020.1733139
- Retamales R., Davies R., Mosqueda G., and Filiatrault A. (2013). Experimental Seismic Fragility of Cold-Formed Steel Framed Gypsum Partition Walls. *Journal of Structural Engineering* 139 (8): 1285–1293. DOI: 10.1080/13632469.2020.1733139
- Rihal S. S. (1982). Behavior of Nonstructural Building Partitions During Earthquakes. *In Proceedings, 7th Symposium on Earthquake Engineering*, India, 10–22 November.
- Serrette R. L., Encalada J., Juadines M., & Nguyen H. (1997). Static Racking Behavior of Plywood, OSB, Gypsum, and Fiberbond Walls with Metal Framing. *Journal of Structural Engineering* 123 (8): 1079-1086. DOI: 10.1061/(ASCE)0733-9445(1997)123:8(1079)
- Taghavi S., and Miranda E. (2003). Response Assessment of Nonstructural Building Elements. Tech. Rep. PEER 2003/05, Pacific Earthquake Engineering Research Center, University of California at Berkeley, Berkeley, CA.
- Wang X., Pantoli E., Hutchinson T.C., Restrepo J.I., Wood R.L., Hoehler M.S., Grzesik P., and Sesma F.H. (2015). Seismic Performance of Cold-Formed Steel Wall Systems in a Full-Scale Building. *Journal of Structural Engineering* 141 (10). DOI: 10.1061/(ASCE)ST.1943-541X.0001245
- Wichman S. (2023). Seismic Behavior of Tall Rocking Mass Timber Walls. Ph.D. Thesis, University of Washington, Seattle.